CrossMark

ORIGINAL ARTICLE

Carbon stable isotopes as indicators of the origin and evolution of CO_2 and CH_4 in urban solid waste disposal sites and nearby areas

Romina Sanci[1] · Héctor Osvaldo Panarello[1]

Abstract Isotopic compositions of CH_4 and CO_2 surface and subsurface gases and groundwater from an urban solid waste disposal site from Gualeguaychú city (Argentina) were measured to detect origin, depth distribution, migration lateral, CH_4 oxidation, and dissolution in groundwater. The highest CH_4 concentrations (60–88 %) with $\delta^{13}C\text{-}CH_4$ (between −60 and −45 ‰) and $\delta^2H\text{-}CH_4$ (between −350 and −260 ‰) were attributed to CH_4 originated by microbial sources, v. gr. acetate fermentation. The $\delta^{13}C\text{-}CO_2$ related to this CH_4 (between −15 and −5.9 ‰) were compatible with this process. Also, the increase of DIC associated to an increase in $\delta^{13}C\text{-DIC}$ values (−12.4, −6.4, −5.8, −1.5, +0.1 and +4 ‰) indicated the transport of dissolved gases (from methanogenesis) in the groundwater flow system. High excess deuterium in 3 piezometers suggests that there were hydrogen isotope exchange between CH_4 and water too. Evidences for CH_4 oxidation were decrease in CH_4 concentrations, shift in C and H isotope ratios of CH_4 to more enriched in the remaining CH_4 (in both, $\delta^{13}C\text{-}CH_4 > -50$ ‰ and $\delta^2H > -260$ ‰) and depletion in ^{13}C of the associated CO_2 (< -20 ‰). Since surface CH_4 and CO_2 concentrations over the covering layer were very low, and the major CH_4 concentrations were found between 60m and 90 cm depth, it is very probable USW has been compacted with low permeability materials (e.g., clay) avoiding large emissions to the atmosphere and creating horizontal barriers within the waste that enable lateral gas migration. Horizontally, it can be seen that these gases migrated outside the disposal site following the topography and that CH_4 disappeared leading to anomalous concentrations of CO_2 whose values are greater than those produced by normal soil respiration. The isotopic value ($\delta^{13}C$) of this CO_2 was also different from that of normal soil respiration (~ -25 ‰) and reflected effects that generated isotopic depletion by diffusion (~ -25 to −32 ‰). The analysis of C isotopes as the main tracer, together H isotopes, has allowed the effective detection of the origin and those secondary processes.

Keywords Methane · Carbon dioxide · Carbon isotopes · Dissolved carbon

Introduction

Urban solid waste disposal sites (USWDS) produce large quantities of gases. The most important ones, methane (CH_4) and carbon dioxide (CO_2), are released by biodegradation processes that act upon the organic fraction of the materials that are disposed. In USWDS without subsoil gas recovery systems, the gases are not exploited and therefore CH_4 and CO_2 are emitted to the atmosphere either by flaring, directly from uncovered waste through top covers, or by migration through the surrounding soil layers as free gases (Christophersen and Kjeldsen 2001). They can even migrate through aqueous phase reaching their dissolution in groundwater or soil water (Kerfoot 1994). The polluting nature of this anthropic source results in the emission of waste products even after its closure and for a time span that can involve years. Hence, in the areas where this kind of activities takes place, it is imperative to evaluate the processes that influence the generation,

✉ Romina Sanci
  romina@ingeis.uba.ar

[1] Instituto de Geocronología y Geología Isotópica (Universidad de Buenos Aires, Consejo Nacional de Investigaciones Científicas y Técnicas), Pabellón INGEIS, Ciudad Universitaria, C1428EHA Ciudad Autónoma de Buenos Aires, Argentina

transport and destination of these gases; especially, taking into account the hazards that they represent to the environment, such as explosions, vegetation damage, contribution to global warming, groundwater pollution and/or changes in its quality due to the presence of carbonic acid (Bjerg et al. 2005).

CH_4 and CO_2 surface emissions (fluxes) have been the subject of numerous environmental studies (ATSDR 2001; Environment Agency UK 2010; SEPA 2004) due to their contribution to greenhouse effect and their possible contribution to global warming (Bogner et al. 2008), especially CH_4 because of its warming potential, twenty-one times greater than that of CO_2. During the last years, quantitative methods (Pumpanen et al. 2004) that enable the measurement of CH_4 and CO_2 emissions at land level in terms of carbon fluxes (C) (Tn/day) have been developed as well as high-resolution portable equipment that allows measuring surface emissions in situ and in an expeditious way. Even if these techniques are time-tested and efficient, when evaluating the impact that these emissions have on the atmosphere, they present some limitations to identify the processes these gases were subjected to, once they were produced: CH_4 oxidation, dissolution in aqueous phase, mixture, diffusive lateral migration in a porous media, etc. Fortunately, the origin of these gases and secondary processes that affect their composition and concentration can be identified by evaluating stable C isotope ratios ($^{13}C/^{12}C$), both in CH_4 and in CO_2

The two main processes that form CH_4 (thermal and microbial decomposition of organic matter) fractionate both C and H isotopes in different degrees, that is why $\delta^{13}C$-CH_4 and δ^2H-CH_4 values are used to discriminate sources of CH_4. Thermogenic CH_4 has a range of $\delta^{13}C$-CH_4 between −55 and −20 ‰, and δ^2H-CH_4 between −250 and −100 ‰ (Whiticar et al. 1986; Whiticar 1999). Biogenic CH_4 presents a further differentiation since this gas is generated from two different metabolic pathways: acetate (and other organic substrates) fermentation and CO_2 reduction. The first group has a $\delta^{13}C$-CH_4 between −65 and −40 ‰ and a δ^2H-CH_4 between −350 and −250 ‰ and the second one, a $\delta^{13}C$-CH_4 between −95 and −60 ‰ and a δ^2H-CH_4 between −240 and −150 ‰ (Coleman et al. 1993; Whiticar et al. 1986). Also, CO_2 records in its isotopic composition all the changes that took place during methanogenesis (Hackley et al. 1996, 1999). These authors pointed out that during the initial phases of aerobic and anaerobic oxidation of organic matter, isotopically light CO_2 is formed (with $\delta^{13}C$-CO_2 values between −30 and −10 ‰, similar in range to those from soil respiration in land ecosystems) being replaced by an isotopically heavy CO_2 as methanogenesis proceeds. The higher levels of CH_4, with $\delta^{13}C$-CO_2 values greater than −10 ‰, are consistent with those

suggested by this authors for a CO_2 generated during this process.

On the other hand, CH_4 formed under anaerobic conditions is oxidized during its transport to the soil surface (0–1 m), into the rhizosphere zone or surficial oxic layers. Bacteria oxidize the ^{12}C-isotope slightly faster than the ^{13}C-isotope; thus, the result is the increase of the $^{13}C/^{12}C$ ratio of the remaining CH_4. Consequently, if CH_4 oxidation occurs, the $\delta^{13}C$ value of the residual CH_4 would become shifted to higher $\delta^{13}C$ values (more enriched than biogenic source). Further, CO_2 produced as a result of CH_4 oxidation can have $\delta^{13}C$ values smaller than −20 ‰ (Conrad et al. 1999). Information on variation in δ^2H of CH_4 shows a shift towards enrichment ($>−260$ ‰), ergo, to more positive values (Chanton et al. 2005).

Another process that could affect the isotopic compositions of both the CO_2 and the CH_4 is fractionation associated with diffusion. Fractionation during this process is caused by differences in the diffusion coefficients of the two isotope species. This effect has been modelled for CO_2 (Cerling 1984) and is relatively small (up to 4.6 ‰ for CO_2) compared to the $\delta^{13}C$ variations observed for CH_4. The stable CH_4 isotopes ($^{12}CH_4$, $^{13}CH_4$ and $^{12}CH_3^2H$) differ in molecular weight and their diffusion coefficient; faster diffusive transport of the lighter isotope resulting in enrichment in the heavier isotope of the remaining gas phase is therefore observed. De Visscher et al. (2004) found that the fractionation factor due to transport, $\alpha_{transport}$, can be as high as 1.0178, due to the difference in molecular diffusion coefficients of CH_4 isotopes ($\varepsilon \approx 18$ ‰).

On the other hand, variations on $\delta^{13}C$-DIC of water can reveal the importance of different biochemical pathways of methanogenesis and CH_4 oxidation (Clark and Fritz 1997). It was remarked that acetate fermentation that occurs chiefly in freshwater environment is responsible for the great fractionation of ^{13}C between CO_2 and CH_4. For CO_2, exchange with groundwater DIC could affect $\delta^{13}C$-DIC pristine values, and DIC tends to get enriched in ^{13}C as methanogenesis takes place in the site. Groundwater DIC can range in $\delta^{13}C$ from −15 to −12 ‰, approximately (Mook 2000; Kerfoot et al. 2003), whereas $\delta^{13}C$-DIC values from methanogenesis can be up to +20 ‰ (Hackley et al. 1996). It should also be considered that this signal is often masked by the simultaneous CH_4 oxidation processes releasing isotope depleted CO_2 to surrounding water. Since CH_4 solubility in water is too low and carbon isotopic fractionation between dissolved CH_4 and gaseous CH_4 is small (<1 ‰), partitioning will have a negligible effect on the C values of the CH_4.

The objective of this work is to detect, using carbon isotopes as the main tracer, the processes involving CH_4 and CO_2 in the study area: origin, depth distribution, lateral

migration, oxidation of CH_4 to form CO_2, and their dissolution in groundwater. Chemical and isotopic data were obtained from the municipal USW disposal site of Gualeguaychú, Entre Ríos, Argentina. Surface and subsurface CH_4 and CO_2 concentrations were determined within the active disposal area and outside the area affected by the USW, together with its isotopic composition ($^{13}C/^{12}C$, $^2H/H$). Physical, chemical and isotopic ($^{13}C/^{12}C$, $^{18}O/^{16}O$, $^2H/H$) parameters of groundwater were analysed to find out if the gases resulting from USW biodegradation altered this matrix.

Study area

The plot of land under study is the Municipal USW disposal site (USWDS) of Gualeguaychú, Entre Ríos, Argentina. The study area is only used for USW disposal. Neither agricultural nor livestock breeding activities are carried out in the site. It is located south of the city, in the vicinity of the confluence of El Cura Stream and the Gualeguaychú River (Fig. 1), that is, on the low area of the stream basin. The flow network obtained from water levels measured in the phreatic aquifer showed that groundwater moves predominantly from SW to NE, coinciding with the regional topographic slope of the El Cura stream basin (Boujon and Sanci 2014). Two reddish-brown loessic levels, called "Pampean sediments" are widely distributed in the basin (Hernandarias Formation and Tezanos Pinto Formation) and hold the phreatic aquifer (Boujon and Sanci 2014).

The disposal site has a filled covered area of approximately 24 ha and an active area of 10 ha, that is in expansion. It has neither subsurface gases nor leachate collection systems. USW accumulates in the depressed areas of the plot since it was originally a quarry (former Irazusta quarry). The active area has a sector where waste was covered and compacted and another which is not covered, where waste is still being accumulated. It has 9 piezometers located up and down the river and across the site (P3, P10, P6, P7, P5, P11, P9, P12, P22), which already existed before this work begun. Gas geochemistry studies made on the inactive area of the disposal site (Sanci et al. 2012) detected that the anomalous emissions corresponded to CO_2 rather than CH_4, with CO_2 fluxes between 31 and 331 g m^{-2} day^{-1} with baseline values due to soil respiration between 29 and 59 g m^{-2} day^{-1} and subsurface CO_2 concentrations of up to 10.3 % (mole fraction × 100) and $\delta^{13}C$ enriched values of up to -17.6 ‰. Hydrochemical and isotopic data from sampling made in October, 2007, showed that as groundwater flowed through the USW disposal site, following the local flow direction (North–South), there was an increase in alkalinity and in the calcite saturation index, and an increase in $\delta^{13}C$ in the total dissolved inorganic carbon, with values ranging between -15 and 4.4 ‰ (Sanci et al. 2012).

Methodology

In September, 2012, a survey of CH_4 and CO_2 of surface and subsurface gases was begun in an active disposal area. To check the occurrence of gas anomalies not previously detected, CH_4 and CO_2 near surface (<4 cm) concentrations were measured using two portable monitors: a micro-FID PHOTOVAC^{TM} for CH_4 (concentration range between 0.1 and 1000 ppm) and an infrared gas analyser (IRGA) Environmental Gas Monitor (EGM-4) PP Systems^{TM} for CO_2 (concentration range between 1 and 20,000 ppm), following the guidelines proposed by environmental agencies from different countries to detect and monitor gases from landfills (ATSDR 2001; Environment Agency UK 2010; SEPA 2004). Although these guidelines are mainly concerned with the study of CH_4—due to its explosion hazard, its major contribution to the greenhouse effect and the possible leaks in gas collection systems or through cracks in the permanent covers—CO_2 was also measured in all sampling campaigns. Surface gases were taken along transects in a SW–NE direction and regularly spaced by 10 m (Fig. 1) and were carried out in the sector where the USW had been covered with fine, compacted materials. Access to the USW expanding open area (without cover) was not possible.

Subsurface gases, generated through biodegradation (production), were quantified in the area surrounding the disposal site (sampling stations labelled G) with an underground subsoil probe that enabled the gas extraction to 30, 60, 90 cm and occasionally 120 cm deep. These concentrations, expressed as molar fraction × 100, were measured in situ with a portable Madur GA21 Plus (measurement range between 0.01 and 4.95 % for CH_4 and CO_2) and by gas chromatography (GC) at the laboratory using a GC HP 5890 Series II with a Thermal Conductivity Detector (TCD) and a Flame Ionization Detector (FID) when concentrations exceeded the upper limit of the portable equipment.

During an October 2013 survey, the study was completed evaluating the probable CH_4 and CO_2 migration towards the adjacent soil. To study migration, not only the screening of free gases at depths 30, 60, 90 and 120 (on S stations, transects T1, T2 and T3, Fig. 1) was done, but also the measurement of free gases accumulated at the headspace of the piezometers. In this case, gases were measured in situ with the Madur GA21 Plus. Additionally and taking into account the hydrodynamic characteristics of the phreatic aquifer, with fluctuating and shallow levels in the
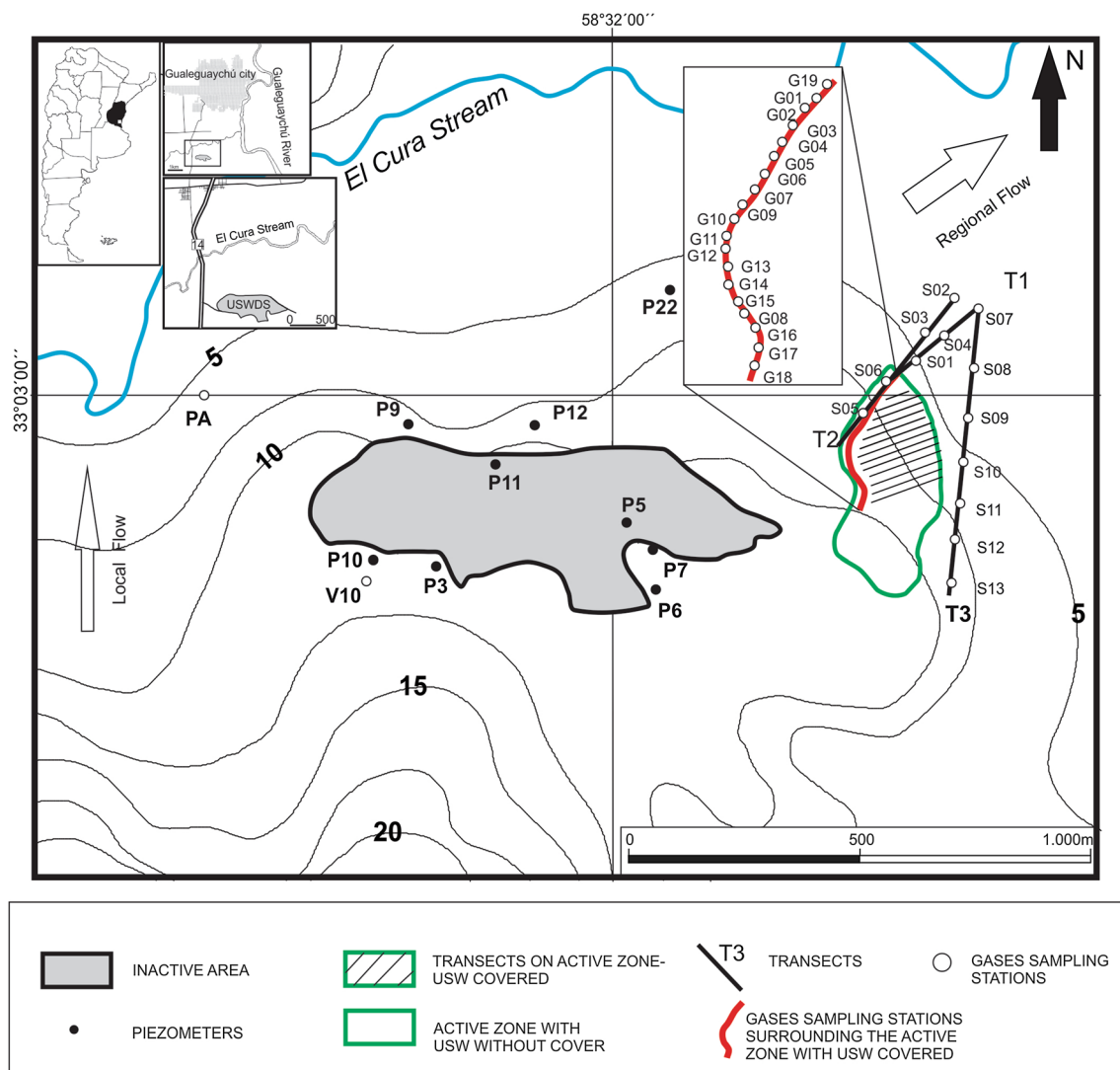
Fig. 1 Location and description of urban solid wastes disposal site (USWDS)

survey area, the water from the piezometers was also sampled to evaluate the possible dissolution of gases in water. Of all the cited piezometers, only P7, P11, P9, P12 and P22 (Fig. 1) were able to be sampled since P3 and P10 were dry at 2.20 and 1.80 m respectively, and P5 and P6 were broken. P3, P10 and P5 were informed in previous works (Sanci et al. 2012). pH, electrical conductivity (EC) and temperature were measured in situ and samples were taken and kept refrigerated until their analysis in the laboratory. Nitrates (NO_3^-), nitrites (NO_2^-) and ammonium (NH_4^+) concentrations were measured with a portable HACH DR/890 photometer. Carbonate (CO_3^{2-}) and bicarbonate (HCO_3^-) determinations were carried out 24 h after receiving the samples by titration with 0.1 N sulphuric acid (H_2SO_4). The concentration of major ions was measured at the Agro-environmental Laboratory at INGEIS: magnesium (Mg^{2+}), calcium (Ca^{2+}), sodium

(Na^+) and potassium (K^+) by atomic absorption spectrometry (Buck Scientific 200A), sulphate (SO_4^{2-}) by inductively coupled plasma atomic emission spectrometry (BAIRD-ICP 2070) and chlorine (Cl^-) by titration with silver nitrate ($AgNO_3$). The concentration of CH_4 dissolved in water was quantified according to the method described in Lomond and Tong (2011). $^{13}C/^{12}C$ isotope ratio from dissolved inorganic carbon (DIC) and $^{18}O/^{16}O$ and $^2H/H$ isotope ratios in water were determined at the INGEIS Stable Isotopes Laboratory. Dissolved organic carbon (DOC) was determined by the SM (standard methods) 5310B analytical technique. Eh values were obtained with PHREEQC (Parkhurst and Appelo 1999) computer code for speciation, batch-reaction, one-dimensional transport and inverse geochemical calculations.

To determine the carbon isotopic composition of CO_2 samples from both campaigns, gases were absorbed with

BaCl$_2$ at pH = 11 (Valencio et al. 2003) and were taken to the laboratory as BaCO$_3$. For CH$_4$, gases were collected in ad hoc bags and processed according to Cordero et al. (2004). DIC from water was precipitated as BaCO$_3$ adding BaCl$_2$ to 100 mL of sample previously adjusted to pH = 11 (Valencio et al. 2003). The precipitates underwent in vacuo heat treatment at 350 °C to remove organic matter interferences and then they were directly introduced into the extraction system. Carbon isotopic ratios ^{13}C/^{12}C were measured on CO$_2$ extracted from carbonates with phosphoric acid (100 %) according to McCrea's (1950), modified by Panarello et al. (1982). The cryogenically purified CO$_2$ was contrasted with an internal reference (Carrara marble). Data were informed as isotopic deviations (δ ‰) relative to the international reference standard Vienna Pee Dee Belemnitella (V-PDB), with an analytical uncertainty of ±0.1 ‰. Isotopic analyses (^{2}H and ^{18}O) were made by laser spectroscopy in a Los Gatos Research (LGR) Liquid Water Isotope Analyzer (OA-ICOS: Off-Axis Integrated Cavity Output Spectroscopy; Wassenaar et al. 2014), at the Stable Isotopes Laboratory of the INGEIS. The reference standard used is the Vienna Standard Mean Ocean Water (V-SMOW). Isotopic results are expressed as δ, defined as δ = 1000(RS–R$_R$)/R$_R$ ‰, where δ is δ^{13}C or δ^{2}H, the isotopic deviation in ‰; S: sample; R: International reference; R: isotopic ratio (^{2}H/^{1}H, ^{18}O/^{16}O, ^{13}C/^{12}C). DOC samples were prepared based on the technique described in Gandhi et al. (2004). Samples were first filtered through 0.45 μm GF/F Acrodisc^{TM} filters. A volume containing about 50 μmol C was transferred to 50 mL beakers (that were previously decontaminated with 50 % nitric acid) and placed in an oven at ca. 50 °C, till dryness. 1 mL of ultra-pure water (UPW) was then added to the sample together with 85 % phosphoric acid (ca. 100–300 μL) and stirred to remove DIC. More UPW was added to reach 2 mL. 150 μL of the concentrated sample was then transferred to tin capsules for liquids in several aliquots. The samples were dried in an oven (ca. 50 °C) after each transfer. The closed capsules were then measured in a Carlo Erba Elemental Analyzer 1180, coupled to a continuous flow Thermo Scientific Delta V mass spectrometer through a Thermo ConFlo IV interface.

δ^{18}O and δ^{2}H values in water were used to detect physical and chemical processes that may cause deviations from the local precipitations isotopic composition. δ^{18}O and δ^{2}H values of precipitations around the world show, in general, a characteristic relationship expressed by the following linear equation: δ^{2}H = 8 δ^{18}O + 10 ‰, known as global meteoric water line (Craig 1961). Since these two isotopic values vary with latitude and climatic conditions, a local meteoric line was calculated taking into account the characteristics of the area under study. The data used were obtained from stations of the National Network for Isotopes

in Precipitation of Argentina (RNC) reporting to the Global Network for Isotopes in Precipitation (GNIP-IAEA-WMO). The nearest ones to the study area are Buenos Aires and Santa Fe. According to Dapeña and Panarello (2007), the local meteoric line for Santa Fe for the 1999–2003 period is δ^{2}H = 8.1 δ^{18}O + 13.1 ‰. In the last years, RNC records indicate that the independent term of the equation has increased to 14 ‰, reaching a value similar to that of the Buenos Aires station, Dapeña and Panarello (2004) i.e., δ^{2}H = 8.0 δ^{18}O + 14.0 ‰. Therefore, this last equation will be used as the Gualeguaychú local meteoric line (LMWL).

Results

Gases

Surface data show CH$_4$ values ranging from 0.1 to 73.6 ppm with mean values between 1.9 and 13.5 ppm (Table 1) for all transects. Likewise, the CO$_2$ concentration range varies between 1 and 68 ppm, with mean values between 2.6 and 16.1 ppm (Table 1). CH$_4$, CO$_2$ and δ^{13}C-CO$_2$ values shown in Fig. 2 correspond to the maximum concentrations found at each sampling station (19 stations labelled G). The depth at which they were observed is also indicated. High CH$_4$ concentrations (between 28.4 and 87.9 %) were present in most stations (G01, G03, G04, G05, G06, G07, G08, G09, G11, G14, G15 and G17), specifically between 60 and 90 cm deep. The associated CO$_2$ shows a smaller concentration (between 2.3 and 4.1 %) with δ^{13}C-CO$_2$ between −32.1 and −0.3 ‰ (Fig. 2). At minor depths, CH$_4$ and CO$_2$ levels reached 1 and 1.8 %, respectively. Stations G18, G16, G13, G12, G10, G02 and G19 did not yield values higher than 10 % for CH$_4$ and 5 % for CO$_2$; δ^{13}C for this CO$_2$ varies between −30.0 and −6.7 ‰.

CH$_4$ and CO$_2$ concentrations of S stations (30, 60, 90 and 120 depth) are represented in Fig. 3, together with δ^{13}C-CO$_2$ data. The highest values found at S05 and S06 sites (CH$_4$ and CO$_2$ of up to 66 and 30 %, respectively), inside the USW disposal site, show the same evolution in depth as that presented in G stations in September 2012, that is, the highest concentrations are found at 60 or 90 cm deep. S stations located outside the active disposal site show a decrease in CH$_4$ (up to 0.4 % and below the detection limit) and CO$_2$ concentrations (up to 10 %). S01, S04 and S07 on T1 transect present low CH$_4$ concentrations—between 0.06 and 0.4 %—(which cannot be discriminated in Fig. 3 because of the chosen axis-scale) and CO$_2$ values that increase with depth and reach up to 6 %. δ^{13}C-CO$_2$ values show a downstream depletion ranging from −27.7 to −31.7 ‰ (60 cm) and from −27.9 to −31.4 ‰ (90 cm).

Table 1 Data show surface CH_4 and CO_2 values for all transects SO–NE; n = stations on each transect

Transects	CH₄				CO₂			
	Min	Max	Media	DesvStd	Min	Max	Media	DesvStd
$n = 19$	0.4	40.7	13.5	11.4	2.0	52.0	16.1	12.8
$n = 20$	0.9	68.0	9.0	14.6	2.0	37.0	8.2	8.5
$n = 21$	0.4	37.7	7.2	9.1	2.0	40.0	10.8	9.4
$n = 22$	0.2	71.3	9.8	18.9	1.0	68.0	11.8	18.7
$n = 21$	0.1	37.8	8.4	11.9	1.0	24.0	7.6	7.0
$n = 19$	0.1	37.2	3.3	8.4	1.0	21.0	4.4	4.5
$n = 19$	0.1	7.5	1.9	2.6	1.0	6.0	2.8	1.4
$n = 19$	0.1	14.6	2.6	3.9	1.0	8.0	3.0	1.8
$n = 7$	1.8	42.5	8.3	15.1	2.0	16.0	5.6	5.3
$n = 13$	1.3	62.1	10.0	19.9	2.0	44.0	11.0	13.2
$n = 11$	1.2	26.4	4.6	7.4	2.0	38.0	9.0	10.6
$n = 16$	1.1	73.6	7.5	17.8	2.0	57.0	8.6	13.9
$n = 14$	1.0	4.3	1.9	0.9	1.0	5.0	2.6	1.2

Fig. 2 Maximum concentrations of CH_4 and CO_2 found at each sampling stations (19 stations labelled *G*) together with $\delta^{13}C$-CO_2 data. The depth at which they were found is also indicated
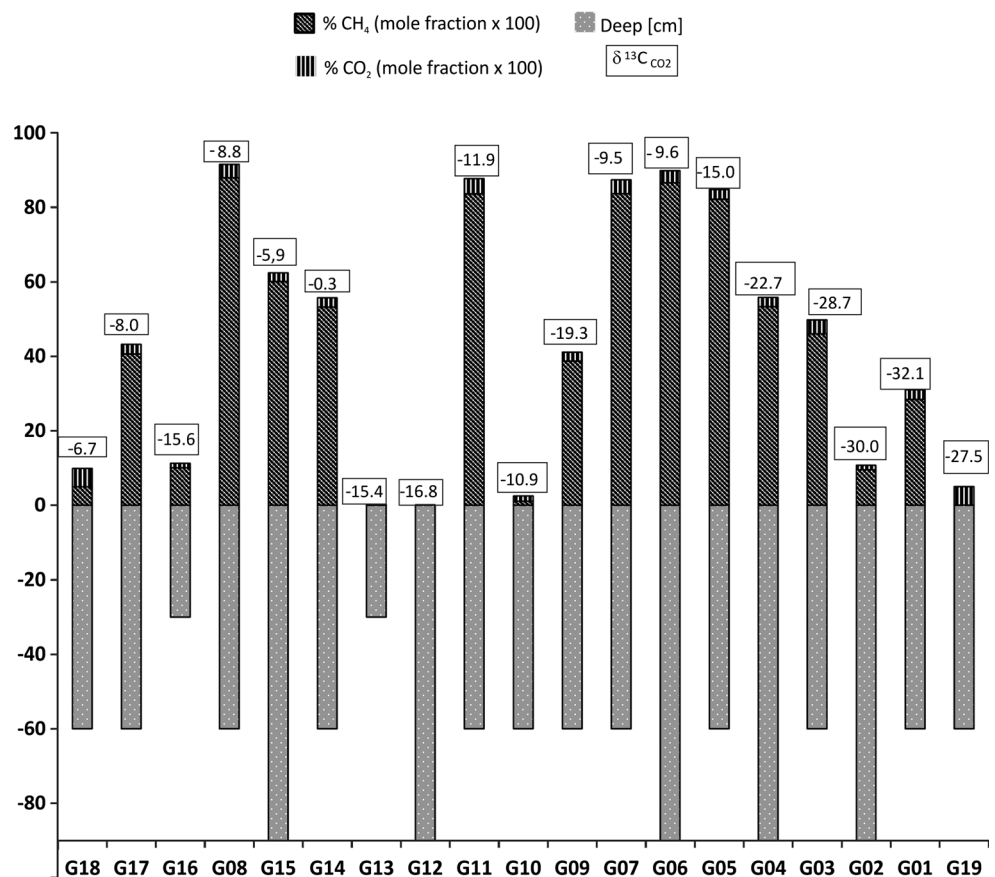
S03 and S02 on T2 transect do not have CH_4. They present CO_2 values that increase with depth (up to 4 %) and a $\delta^{13}C$-CO_2 value at 60 cm of between -20.4 and -24.2 ‰ going downstream and at 90 cm, between -18.1 and -16.3 ‰. Transect T3 (S13, S12, S11, S10, S09, S08,

S07), with a N–S direction (coinciding with the local flow network), presents the highest subsurface CO_2 values (up to 10 %), with the exception of S08-90 cm where the probe was found clogged; the CH_4 detected in some stations is minimal (between 0.01 and 0.13 %) and the $\delta^{13}C$-CO_2
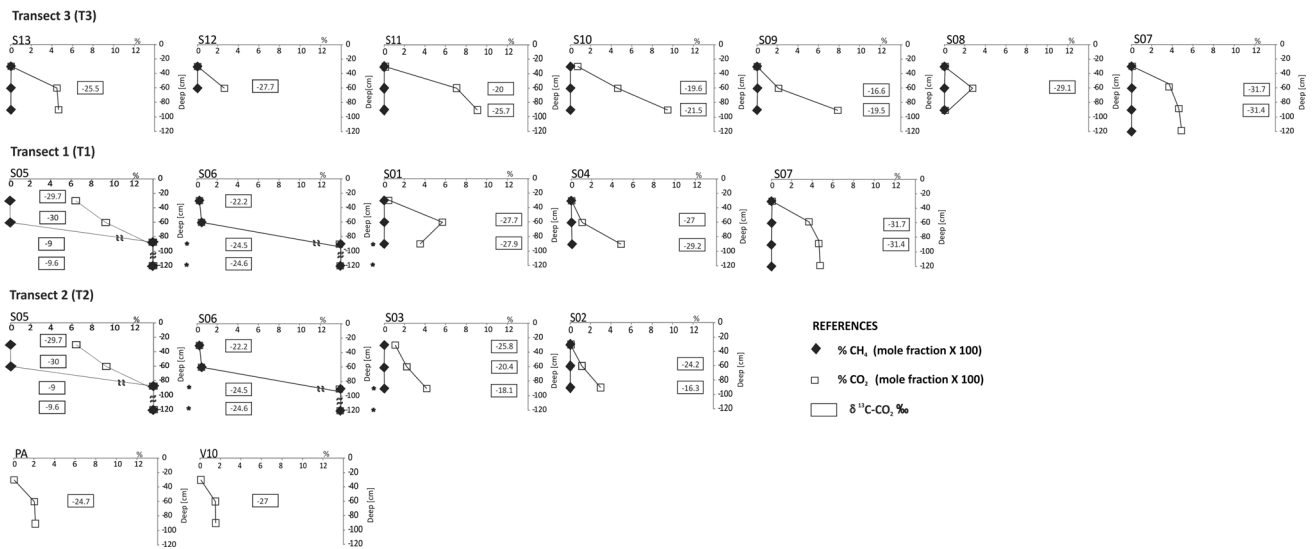
Fig. 3 CH_4 and CO_2 concentrations at all studied depths (30, 60, 90 and 120 cm) and $\delta^{13}C$-CO_2 data of soundings made on transects T1, T2 y T3. PA and V10 are reference values of soil respiration. *Asterisk* S05-90 y S05-120 cm, y S06-90 y S06-120 cm (see CH_4 y CO_2 concentrations in Table 2)

value varies between −31.7 and −16.6 ‰. PA and V10, two stations placed upstream waste disposition, show a stable CO_2 concentration of 2 % from 60 cm downwards, attributed to a normal soil respiration, opposite to S stations located outside the disposal that show a gradual increase in CO_2 concentration with depth. Also, PA and V10 present a $\delta^{13}C$-CO_2 between −27 and −24.7 ‰, a more confined range than the $\delta^{13}C$-CO_2 from all S stations, which range from −31.7 to −9 ‰.

Concerning the origin of CH_4, Table 2 shows the isotopic data of C and H from CH_4 and the $\delta^{13}C$ from its associated CO_2 from 12 samples situated in the area surrounding the disposal site (eight samples from September 2012 and four from October 2013). $\delta^{13}C$-CH_4 and δ^2H-CH_4 values range from −61.7 to −42.5 ‰, and from −309 to −199 ‰, respectively. $\delta^{13}C$ values from CO_2 range from −32.1 to −8.8 ‰. $\delta^{13}C$-CH_4 versus δ^2H-CH_4 data presented in Fig. 4a show that four samples (G01−60, G03−60, G07−60 and G09-60) fall within the field of thermogenic gas, out of which G01-60, G03-60 and G09-60 appear in Fig. 4b under the "oxidation effects" of CH_4, outside the field of landfill gases. Three other samples (G06-90, G15-90 and S05-120) plot in the field of gases of mixed origin (from microbial and thermogenic origin) and five other samples (G08-60, G11-60, S05-90, S06-90 and S06-120) are from microbial origin due to acetate fermentation. The position of the samples in Fig. 4b ($\delta^{13}C$-CO_2 vs. $\delta^{13}C$-CH_4) indicates that the majority of them correspond to landfill gases which were the product of acetate fermentation, with a tendency towards CH_4 oxidation.
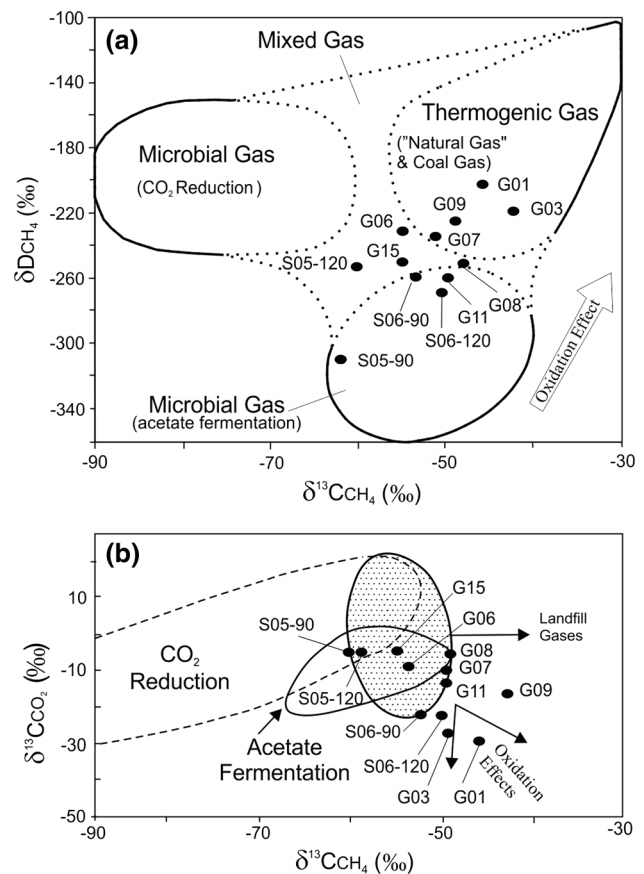

Fig. 4 a Plot of $\delta^{13}C$ and δ^2H of methane (Table 2) showing the areas with different sources of methane. **b** Plot of $\delta^{13}C$ of methane and carbon dioxide (Table 2) showing the areas with different biogenic sources, including typical plot of landfill gases and oxidation effects. Source: Whiticar et al. (1986) and Coleman et al. (1993)

Table 2 Isotopic data of C e H from CH_4, and $\delta^{13}C$-CO_2 associated from 12 samples collected in the unsaturated zone and situated in the area surrounding the disposal site (8 samples from September 2012 labelled G, and 4 samples from October 2012 labelled S)

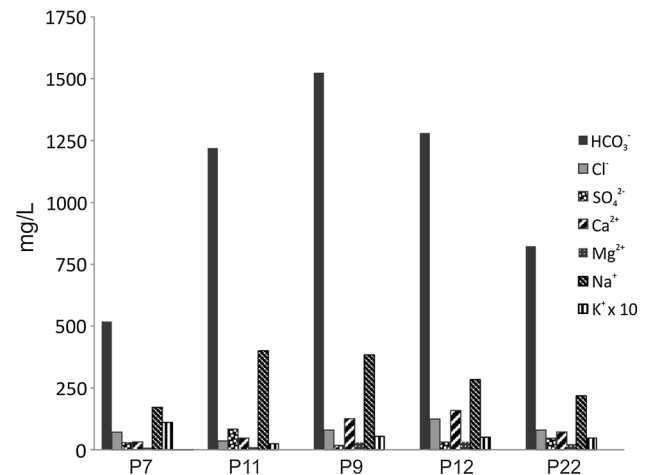| Muestra	δ^2H-CH_4 (‰)	$\delta^{13}C$-CH_4 (‰)	$\delta^{13}C$-CO_2 (‰)	XCH_4 (%)	XCO_2 (%)
G01-60	−199	−46.4	−32.1	28.4	2.6
G03-60	−223	−48.9	−28.7	46.1	3.7
G06-90	−236	−54.1	−9.6	86.6	3.2
G07-60	−235	−49.5	−9.5	83.7	3.7
G08-60	−246	−47.4	−8.8	87.9	3.6
G09-60	−221	−42.5	−19.3	38.7	2.4
G11-60	−258	−49.2	−11.9	83.6	4.1
G15-90	−250	−54.9	−5.9	60.1	2.3
S05-90	−309	−61.7	−9	66.1	29.0
S05-120	−253	−60.2	−9.6	64.7	28.1
S06-90	−259	−53.5	−24.5	42.1	30.0
S06-120	−265	−50.1	−24.6	28.8	20.1

Groundwater

Groundwater levels recorded in the piezometers P7, P11, P9, P12 and P22 were between 30 and 70 cm (Table 3) with the exception of P3 and P10 that were found dry at 2.20 and 1.80 m, respectively. These piezometers were considered references in previous works (Sanci et al. 2012). Table 3 also includes the data of CO_2 concentration in the headspace of all piezometers (CH_4 as free gas was not detected in any of them) as well as pH, EC and temperature values measured in the field. Based on the chemical results of HCO_3^-, Cl^-, SO_4^{2-}, Ca^{2+}, Mg^{2+},

Fig. 5 Graphical presentation of chemical data from groundwater samples (major elements)

Na^+ and K^+ (Fig. 5), it can be observed that the predominant ion in all samples is HCO_3^-, while cations are mainly represented by Na^+. Table 4 presents the concentrations of redox species NO_3^-, NO_2^-, NH_4^+, DOC, total Fe, total Mn, Fe^{2+}, and dissolved CH_4, which are plotted in Fig. 6a, c along two local groundwater flow lines (North–South). In both of them, there is a downstream tendency showing a decrease in DOC, NH_4^+ and total Fe and an increase in NO_3^- and total Mn. Concentrations of dissolved Fe^{2+} and CH_4 were null. The Eh from the NO_2^-/NO_3^- redox pair calculated with the PHREEQC program varies between 0.413 and 0.460 volts (Table 4). The ion balance error was between −10.77 and −14.69 %. $\delta^{13}C$-DOC and $\delta^{13}C$-DIC values are presented

Table 3 pH, electrical conductivity, temperature, deep water and CO_2–CH_4 concentrations of headspace from piezometers

Well	pH	EC (μS/cm)	T (°C)	Deep water (cm)	CO_2 headspace (%)	CH_4 headspace (%)
P7	7.51	970	17.4	70	2.84	0
P11	7.28	1580	18.5	40	2.1	0
P9	6.99	2040	17.2	30	2.97	0
P12	6.99	1850	19.3	30	2.63	0
P22	7.6	1320	17.3	30	2.43	0

Table 4 Concentrations of redox species and Eh from the NO_2^-/NO_3^- redox pair calculated with PHREEQC

POZO	NO_3^- (mg/L)	NO_2^- (mg/L)	NH_4^+ (mg/L)	DOC (mg/L)	Fe total (mg/L)	Mn total (mg/L)	Fe^{2+} (mg/L)	CH_4 (mg/L)	Eh (volts)
P7	0	0	0.77	18.5	1.1	0.7	0	0	ND
P11	0.9	3	0.04	14.2	0.01	1	0	0	0.413
P9	3.3	1	0.01	13.1	0.02	1.5	0	0	0.460
P12	1.7	2	0	17.2	0.01	1	0	0	0.439
P22	4.8	3	0.28	11	0.03	1.4	0	0	0.416

Fig. 6 Plot of redox species concentration along two local groundwater *flow lines* (north–south)

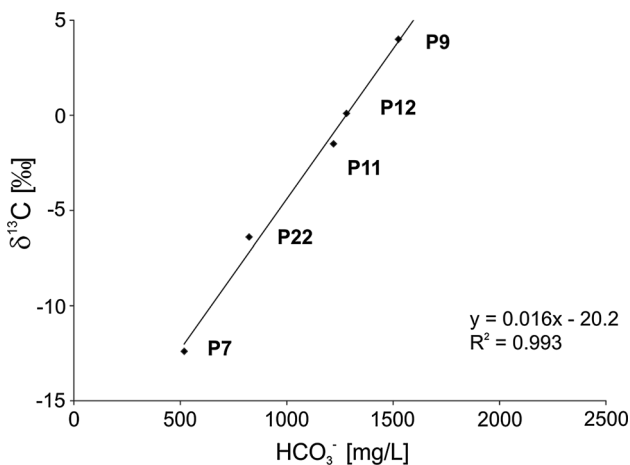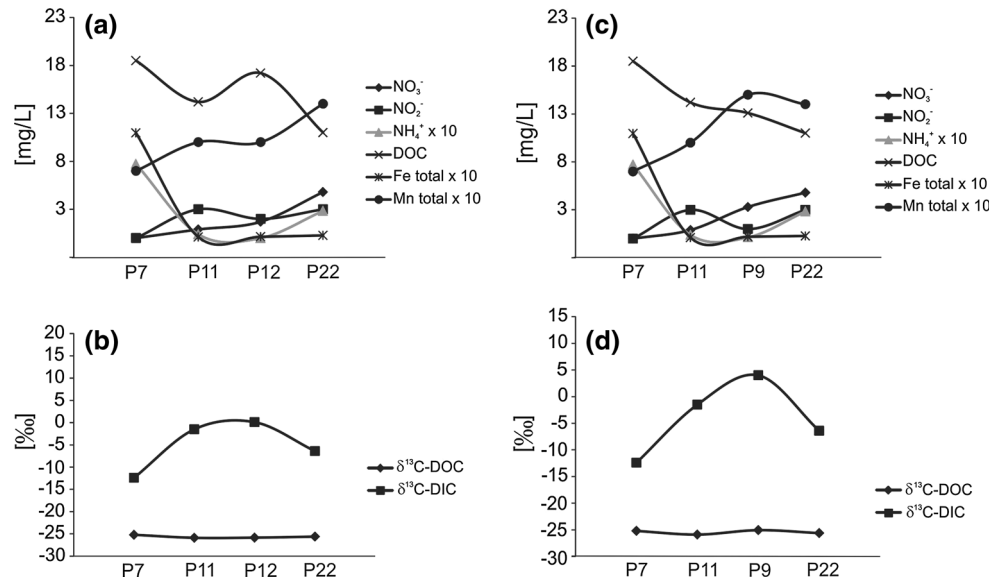**Fig. 7** Linear correlations between HCO_3^- content and $\delta^{13}C$-DIC

in Fig. 6b, d along the two local groundwater flow lines, showing no change for the first parameter and an increase in the second one. DOC presents a decreasing tendency as it flows downstream (Fig. 6) with $\delta^{13}C$-DOC values remaining constant (values around -24 ‰), which would indicate the presence of another process that accounts for DOC decrease or small isotope effect associated to degradation of DOC. Also, there are a positive linear correlation between HCO_3- content and $\delta13C$-DIC ($R^2 = 0.993$) for samples P7–P22–P11–P12–P9 (Fig. 7). Figure 8 shows δ^2H values (between -39 and -27 ‰) vs. $\delta^{18}O$ (between -6.5 and -5.2 ‰) obtained from P7, P11, P9, P12 and P22 piezometers and regional isotope composition of a mill network producing for the water table and surface waters sampled within the Cura stream

basin (Boujon and Sanci 2014) together with the local meteoric water line (LMWL). While it is true that the samples have a meteoric origin due to its proximity to the LMWL, it can be seen also that some samples are enriched in deuterium: P9, P11 and P12.

Discussion

The samples represented in Fig. 4a, with $\delta^{13}C$-CH_4 and δ^2H-CH_4, fall inside the microbial gas-fermentation acetate, mixed gases and thermogenic fields. The first one is characteristic of landfill gases with $\delta^{13}C$-CH_4 values between -60 and -45 ‰ and δ^2H-CH_4 between -350 and -260 ‰ (Coleman et al. 1993; Hackley et al. 1996), and similar to CH_4 produced in natural freshwater environments (Hornibrook et al. 2000). Stations with high CH_4 concentrations (Table 2) have more enriched than $\delta^{13}C$-CO_2 soil respiration values (between -19 and -9 ‰), suggesting their relationship with the methanogenesis process. Soil respiration, meaning the total production of CO_2 coming from the respiration of soil organisms and roots (Lloyd and Taylor 1994), has an average isotopic value $\delta^{13}C$ of -23 ‰ (for C3 plants) and of -9 ‰ (for C4 plants), with extreme CO_2 concentrations between 0.3 and 3 % (Clark and Fritz 1997). According to these authors, ca 85 % of the terrestrial plants that inhabit terrestrial landscapes are C3, since C4 are characteristic of particular areas or areas cultivated with corn, sorghum, sugar cane, etc., it is not unusual to find $\delta^{13}C$-CO_2 soil respiration values around -23 ‰. Thus said, $\delta^{13}C$-CO_2 values higher than -23 ‰ would show that USW biodegradation processes are active. This pattern can be observed in Fig. 2:
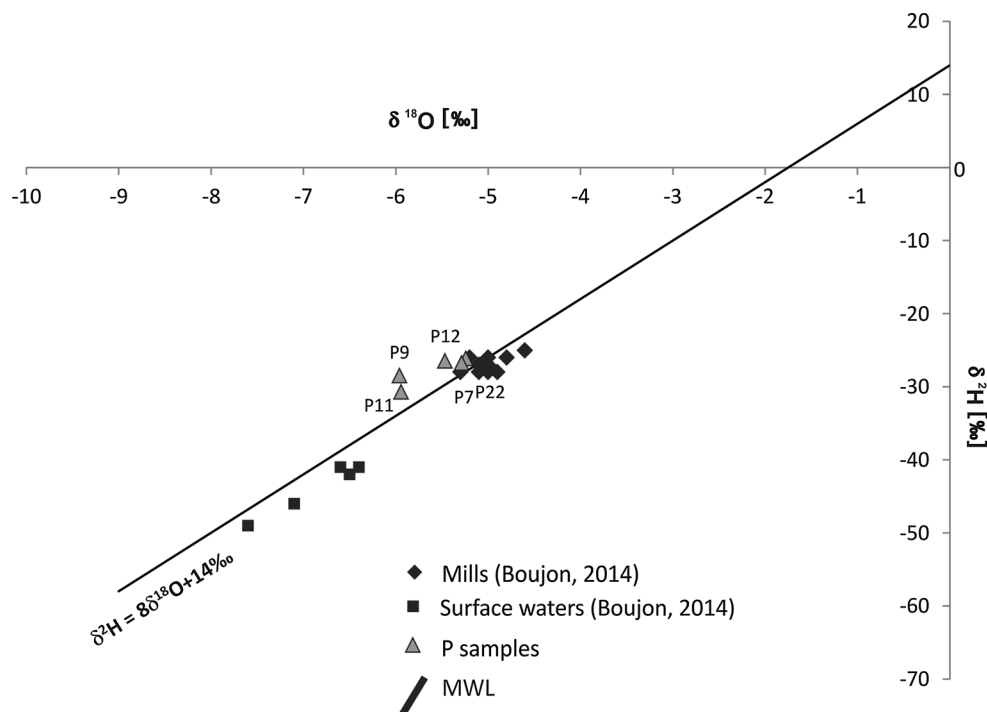
Fig. 8 Plot of δ^2H and $\delta^{18}O$ values from groundwater samples on meteoric water line (MWL)

CH_4 levels between 60 and 88 % (stations G05, G06, G07, G08, G11 and G15) have $\delta^{13}C\text{-}CO_2$ values between -15 and -5.9 ‰, which are consistent with methanogenesis process.

CH_4 oxidation to form CO_2 showed a distinctive and opposite isotopic signature: $^{13}C\text{-}CO_2$ decreases, whereas ^2H and ^{13}C of the residual CH_4 are enriched so the values can be mistaken as a "thermogenic source" (Whiticar 1999). This is observed in Fig. 4a where most of the samples present a trend towards an isotopic enrichment of $^{13}C\text{-}CH_4$ (>50–55 ‰) and $^2H\text{-}CH_4$ (>-260 ‰). As it happens in Rayleigh processes, the products (CO_2 and water) tend to take the light isotopes leaving the remaining CH_4 more enriched (Clark and Fritz 1997). This can also be seen in Fig. 4b where $\delta^{13}C\text{-}CH_4$ and $\delta^{13}C\text{-}CO_2$ are plotted: for samples falling outside landfill, gases have values more enriched than -50 ‰ in $\delta^{13}C\text{-}CH_4$ and more depleted than -20 ‰ in $\delta^{13}C\text{-}CO_2$. Some authors (Bergamaschi 1997; Coleman et al. 1981; Mahieu et al. 2008) reported enrichment factors (ε) due to CH_4 oxidation between 3 and 31 ‰, which is consistent with the values found for the CH_4 source and its oxidization product. Another way of detecting this process is plotting CH_4 concentration (%) vs. the $\delta^{13}C\text{-}CO_2$ of its associated CO_2. In Fig. 9, a weak linearity can be observed between data ($R^2 = 0.678$), although the lower CH_4 concentrations seem to be more strongly linked to the more depleted $\delta^{13}C\text{-}CO_2$ values (smaller than -20 ‰), and the higher CH_4 concentrations, to the more enriched ones.
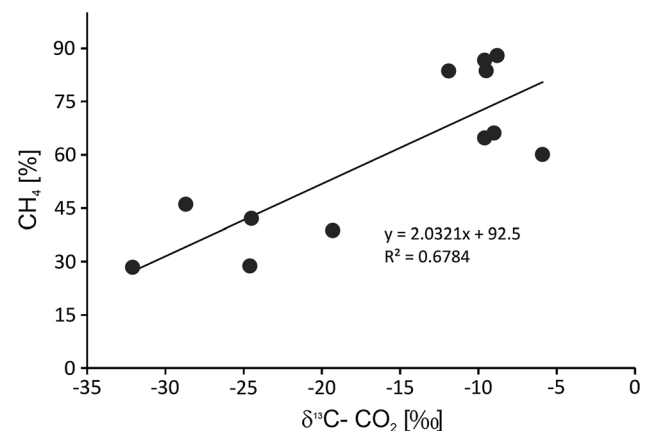

Fig. 9 Plot of CH_4 concentration and associated $\delta^{13}C\text{-}CO_2$ from Table 2 data

S05 station shows clearly how oxidation takes place vertically: signs of biodegradation by acetate fermentation at deepest levels (90 and 120 cm) present $\delta^{13}C\text{-}CO_2$ values around -9 ‰ that are depleted up to -30 ‰ towards the soil–air interface (Fig. 3). This is consistent with the surficial oxic layers of subsoil and rhizosphere zone, which allows the input of air into the system and CH_4 consumption. In USWDS, no adequate engineering practices exist, but the very low CH_4 and CO_2 surface emissions and high CH_4 concentrations accumulated at 60 and 90 cm depth suggest USW has been compacted with low permeability materials (e.g., clay). In the last decades, this

material was usually used as a daily cover to minimize the leachate production at sites without recovery systems. This can create horizontal barriers within the waste that enable lateral gas migration, especially at sites without liners (Christophersen and Kjeldsen 2001). Then, the pressure that gases generate in disposal sites may cause their transportation to the unsaturated zone adjacent to the waste disposal site. CH_4 and CO_2 sampled to different depths 30–60–90 (120) cm (S stations) have been studied in 3 transects T1, T2 and T3 located outside the USWDS. T1 and T2 only comprise 2 sampling stations (S05 y S06) in the active deposition area of USWDS. All results are presented in Fig. 3. It can be seen that CH_4 tended to disappear (or actually disappears) outside of active area and CO_2 and $\delta^{13}C$-CO_2 values obtained were different chemically and isotopically from those from normal soil respiration. For this case, PA and V10 values (taken as reference) presented CO_2 concentrations around 2 % at 60 and 90 cm deep and a $\delta^{13}C$-CO_2 value between −27 and −24.7 ‰, consistent with those mentioned above for C3 plants.

In transect T1 and T2, S05 and S06 show active production of CH_4 in the two deeper layers (90–120 cm) and the upper layers do not contain CH_4 probably due to vertical migration and oxidation. S01, S04 y S07 exhibit anomalous CO_2 concentration (much higher than those due to soil respiration) due to lateral CO_2 migration from the active zone. $\delta^{13}C$ values more depleted ($\delta^{13}C$-CO_2 −27.9, −29.2 and −31.4 ‰) in the flow direction support the existence of a horizontal diffusive process. A similar pattern is observed in S03 and S02 in transect T2, but in this case the trend to depletion in ^{13}C is not the same, probably vertical migration is proceeding in this two stations with isotopically depleted CO_2 flowing upwards leading the deeper CO_2 relatively more enriched.

T3 presents high concentrations of CO_2 as the result of lateral migration from the adjacent zone. Since the most probable flux direction would be SW–NE, S13 and S11 would not receive the whole flux because they are not directly in the flow path from the active zone. In addition, the expansive active zone is not covered in this section allowing produced CO_2 to escape to the atmosphere. $\delta^{13}C$ values decrease with the distance to the source suggesting a fractionation by diffusion. S11 to S07 show an evolution with horizontal transport in the level 90 cm with variable contribution from level 90 cm to level 60 cm. The evolution is not smooth due to marked differences in the soil; however, a systematic fractionation leads the isotopic composition from −25 to −31.7 ‰, averaging the two levels confirming the bidimensional (lateral + vertical) diffusion mechanism.

The solubility of a gas in a liquid is controlled by Henry's Law. In equilibrium, Henry's constants for CH_4 and CO_2 are 29 and 1.1, respectively. Therefore, a major proportion of CO_2 would be captured by water before CH_4 is absorbed (Kerfoot 1994). In piezometers P7, P9, P11, P12 and P22, no dissolved CH_4 in groundwater was found but it was found, indeed, an increase of HCO_3^- associated to an increase in $\delta^{13}C$-DIC values (−12.4, −6.4, −5.8, −1.5, +0.1 and +4 ‰) (Fig. 7a). Based on the high concentrations of DIC measured in the groundwater samples, it is clear that a significant proportion of the CO_2 isotopically enriched is stored in the groundwater as DIC. This happens because there is transport of dissolved gases in the groundwater flow system, with a CO_2 enriched in the ^{13}C by acetate fermentation. This trend is typical for methanogenesis and some authors (Coleman et al. 1993; Hackley et al. 1996; van Breukelen et al. 2003) reported $\delta^{13}C$-DIC values significantly more positive (between +1 and +20 ‰) than those from pristine groundwater (between −15 and −12 ‰).

In respect to water isotope composition (Fig. 8), the piezometers' and mills samples fit around the LMWL; however, P9, P11 and P12 show relatively elevated deuterium excess ($d = \delta\ ^2H - 8\ \delta\ ^{18}O$) values that can be related to hydrogen isotope exchange between water and CH_4. Anomalous values of d for these piezometers indicate mixing or isotopic exchange with other sources. This relative enrichment in ^2H was observed during methanogenesis process without affecting the oxygen isotopic composition and thus increasing the value of d (Castañeda et al. 2012). Isotopic fractionation occurs with the preferential association of lighter hydrogen isotope with the gas phase, CH_4, leaving the heavier isotope in the liquid one. This fact, joined to the high values of $\delta^{13}C$-DIC (4, −1.5 and 0.1 ‰ for P9, P11 and P12, respectively) would confirm that methanogenesis process.

Conclusions

The analysis of C isotopes has allowed the effective detection of the origin and those secondary processes that derive from the migration of gases to atmosphere and nearby areas. Chemical and isotopic data from CH_4 and CO_2 gases, obtained from the subsoil of the active part of the USWDS, are consistent with a methanogenesis process. The highest CH_4 concentrations (between 60 and 88 %) have $\delta^{13}C$-CH_4 (between −60 and −45 ‰) and δ^2H-CH_4 (between −350 and −260 ‰) are attributed to CH_4 originated by microbial sources, v. gr. acetate fermentation. The $\delta^{13}C$ of CO_2 gas found together with this CH_4 (between −15 and −5.9 ‰) are compatible with this process. Also, the increase of DIC associated to an increase in $\delta^{13}C$-DIC values (−12.4, −6.4, −5.8, −1.5, +0.1 and +4 ‰) suggests the transport of dissolved gases in the groundwater flow system. As CH_4 is formed by acetate

fermentation, the CO_2 is enriched in ^{13}C and then it is incorporates to DIC. High excess deuterium in 3 piezometers suggests that there were hydrogen isotope exchange between CH_4 and water too.

Isotopic evidence and geochemical indicators for CH_4 oxidation in the active area are decrease in CH_4 concentrations, shift in C and H isotope ratios of CH_4 to more enriched in the remaining CH_4 (in both, $\delta^{13}C$-CH4 > -50 ‰ and $\delta^2H > -260$ ‰) and depletion in ^{13}C of the associated CO_2 (< -20 ‰). Since surface CH_4 and CO_2 concentrations over the covering layer were very low, and the major CH_4 concentrations were found between 60 and 90 cm depth, it is very probable USW has been compacted with low permeability materials (e.g., clay), avoiding large emissions to the atmosphere and creating horizontal barriers within the waste that enable lateral gas migration. Horizontally, it can be seen that these gases migrated outside the disposal site following the topography and that CH_4 disappeared leading to anomalous concentrations of CO_2 whose values are greater than those produced by normal soil respiration. The isotopic value ($\delta^{13}C$) of this CO_2 was also different from that of normal soil respiration (~ -25 ‰) and reflected effects that generated isotopic depletion by diffusion (-25 to -32 ‰).

References

ATSDR (2001) Agency for toxic substances and disease registry. Landfill gas primer—an overview for environmental health professionals. http://www.atsdr.cdc.gov/HAC/landfill/html/intro.html

Barlaz MA, Green RB, Chanton JP, Goldsmith CD, Hater GR (2004) Evaluation of a biologically active cover for mitigation of landfill gas emissions. Environ Sci Technol 38:4891–4899

Bergamaschi P (1997) Seasonal variations of stable hydrogen and carbon isotope ratios in methane from a Chinese rice paddy. J Geophys Res 102(D21):25383–25393

Bjerg PL, Albrechtsen HJ, Kjeldsen P, Christensen TH (2005) The groundwater geochemistry of waste disposal facilities. In: Sherwood Lollar B (ed) Environmental geochemistry Vol. 9. Treatise on geochemistry. Elsevier–Pergamon, Oxford, pp 579–612

Bogner J, Pipatti R, Hashimoto S, Diaz C, Mareckova K, Diaz L, Kjeldsen P, Monni S, Faaij A, Gao Q (2008) Mitigation of global greenhouse gas emissions from waste: conclusions and strategies from the intergovernmental panel on climate change (IPCC). Fourth assessment report. Working group III (Mitigation). Waste Manag Res 26:11–32

Boujon P, Sanci R (2014) Evaluación de la vulnerabilidad del acuífero libre en la cuenca del Arroyo El Cura, Gualeguaychú. Entre Ríos Rev Asoc Geol Arg 71(2):274–289

Castañeda SS, Sucgang RJ, Almoneda RV, Mendoza ND, David CPC (2012) Environmental isotopes and major ions for tracing leachate contamination from a municipal landfill in Metro Manila, Philippines. J Environ Radioact 110:30–37

Cerling TE, Solomon DK, Quade JB, John R (1991) On the isotopic composition of carbon in soil carbon dioxide. Geochim Cosmochim Acta 55(11):3403–3405

Chanton LC, Chasar P, Glaser D, Siegel (2005) Carbon and hydrogen isotope effects in microbial methane from terrestrial environments. In: Flanagan LB, Ehleringer JR, Pataki DE (eds) Stable isotopes and biosphere–atmosphere interactions, physiological ecology series. Elsevier–Academic Press, Amsterdam, pp 85–105 **Chapter 6**

Christophersen M, Kjeldsen P (2001) Lateral gas transport in soil adjacent to an old landfill: factors governing gas migration. Waste Manage Res 19:144–159

Clark ID, Fritz M (1997) Tracing the carbon cycle. In: Environmental isotopes in hydrogeology, Lewis Publishers, New York, pp 111–136

Coleman DD, Risatti BJ, Schoell M (1981) Fraction of carbon and hydrogen isotopes by methane oxidizing bacteria. Geochim Cosmochim Acta 45:1033–1037

Coleman DD, Liu CL, Hacley KC, Benson LJ (1993) Identification of landfill methane using carbon and hydrogen isotope analysis. In: Proceedings of 16th international madison waste conference, municipal & industrial waste, Department of Engineering Professional Development, University of Wisconsin, Madison, pp 303–314

Conrad ME, Templeton AS, Daley PF, Alvarez-Cohen L (1999) Isotopic evidence for biological control on migration of petroleum hydrocarbons. Org Geochem 30:843–859

Cordero R, Panarello HO, Corvalán C, Galante G, Ostera HA (2004) Determinación experimental de 13C y 2H sobre metano. XXV Congreso Argentino de Química (resumen), Facultad de Ingeniería-UNCPBA, Olavarría, Buenos Aires

Craig H (1961) Isotopic variations in meteoric water. Science 133:1702–1703

Dapeña C, Panarello HO (2004) Composición isotópica de la lluvia de Buenos Aires. Su importancia para el estudio de los sistemas hidrológicos pampeanos. Revista Latino-Americana de Hidrogeología 4:17–25

Dapeña C, Panarello HO (2007) Estación Santa Fe. Red Nacional de Colectores, Argentina, V Congreso Argentino de Hidrogeología, Paraná, Entre Ríos, IAH Universidad Nacional de Entre Ríos, pp 187–198

De Visscher A, De Pourcq I, Chanton J (2004) Isotope fractionation effects by diffusion and methane oxidation in landfill cover soils. J Geophys Res 109:D18111. doi:10.1029/2004JD004857

Environment Agency UK (2010) Guidance on the management of landfill gas. http://www.environment-agency.gov.uk/business/sectors/108918.aspx#landfillgas

Gandhi H, Wiegner TN, Ostrom PH, Kaplan LA, Ostrom NE (2004) Isotopic (13C) analysis of dissolved organic carbon in stream water using an elemental analyzer coupled to a stable isotope ratio mass. Rapid Commun Mass Spectrom 18:903–906

Gat JR (2010) Isotope hydrology. A study of the water cycle. Centre for Environmental Technology. Imperial College, London, pp 70–71

Hackley KC, Liu CL, Coleman DD (1996) Environmental isotope characteristics of landfill leachates and gases. Ground Water 34(5):827–836

Hackley KC, Liu CL, Traidor D (1999) Isotopic identification of the source of methane in subsurface sediments of an area surrounded by waste disposal facilities. Appl Geochem 14:119–131

Hornibrook ERC, Longstaffe FJ, Fyfe WS (2000) Evolution of stable carbon isotope compositions for methane and carbon dioxide in freshwater wetlands and other anaerobic environments. Geochim Cosmochim Ac 64(6):1013–1027

Kerfoot HB (1994) Landfill gas effects on groundwater samples at a municipal solid waste facility. J Air Waste Manage Assoc 44:1293–1298

Kerfoot HK, Baker JA, Burt DM (2003) The use of isotopes to identify landfill gas effects on groundwater. J Environ Monit 5:896–901

Kjeldsen P, Morton A, Barlaz A, Rooker P, Baun A, Ledin A, Christensen TH (2002) Present and long-term composition of MSW landfill leachate: a review. Crit Rev Environ Sci Technol 32(4):297–336

Kumar S, Mondal AN, Gaikwad SA, Devotta S, Singh RN (2004) Qualitative assessment of methane emission inventory from municipal solid waste disposal: a case study. Atmos Environ 38:4921–4929

Lloyd J, Taylor JA (1994) On the temperature dependence of soil respiration. Funct Ecol 8:315–323

Lomond JS, Tong AZ (2011) Rapid analysis of dissolved methane, ethylene, acetylene and ethane using partition coefficients and headspace-gas chromatography. J Chromatogr Sci 49:469–475

MacCrea JM (1950) On the isotopic chemistry of carbonates and paleotemperature scale. J Chem Phys 18(6):849–857

Mahieu K, De Visscher A, Vanrolleghem PA, Van Cleemput O (2008) Modelling of stable isotope fractionation by methane oxidation and diffusion in landfill cover soils. Waste Manag 28:1535–1542

Mook WG (2000) Environmental isotopes in the hydrological cycle. In: Mook WG (ed) Principles and applications, vol I. UNESCO, Paris, pp 96–101

Panarello HO, Garcia CM, Valencia SA, Linares E (1982) Determinación de la composición isotópica del carbono en carbonatos, su utilización en Hidrogeología y Geología. Rev Asoc Geol Arg XXXV(4): 460–466

Panarello HO, Dapeña C, Ostera HA, Stöckli F (2005) Caracterización química e isotópica preliminar del Basurero Municipal de Gualeguaychú, provincia de Entre Ríos, República Argentina. IV Congreso Argentino de Hidrogeología, Río Cuarto, Universidad Nacional de Río Cuarto, 197–205

Parkhurst DL, Appelo CAJ (1999) User's guide to PHREEQC—a computer program for speciation, batch reaction, one-dimensional transport, and inverse geochemical calculations. Water Resour Invest Rep 99-4259 US Geol Surv, Denver

Pumpanen J, Kolari P, Lvesniemi H, Minkkinen K, Vesala N, Lohila A, Larmola T, Morero M, Pihlatie M, Janssens I, Yuste JC, Grünzweig JM, Reth S, Subke J, Savage K, Kutsch W, Ǿ Streng G, Ziegler W, Anthoni P, Lindroth A, Hari P (2004) Comparison of different chamber techniques for measuring soil CO2 efflux. Agric For Meteorol 123:159–176

Sanci R, Panarello HO, Ostera HA (2012) CO2 emissions from a municipal site for final disposal of solid waste in Gualeguaychu, Entre Rios Province, Argentina. Environ Earth Sci 66:519–528

SEPA (2004) Scottish environment protection agency. Guidance on the management of landfill gas. http://www.sepa.org.uk/waste/waste_regulation/landfill.aspx

Stumm W, Morgan JJ (1996) Aquatic chemistry. Environmental Science and Technology, New York, p 461

Valencio S, Ostera HA, Panarello H (2003) Monitoring 13C in CO2 soil gas from a landfill: first results from a case study. IV South American symposium on isotope geology, Short papers I: 128–130, Salvador, Brasil

Van Breukelen BM, Roling FM, Groen J, Griffioen J, Van Verseveld HW (2003) Biogeochemistry and isotope geochemistry of a landfill leachate plume. J Contam Hydrol 65:245–268

Wassenaar LI, Coplen TB, Aggarwal PK (2014) Approaches for achieving long-term accuracy and precision of δ18O and δ2H for waters analyzed using laser absorption spectrometers. Environ Sci Technol 48(2):1123–1131

Whiticar MJ (1999) Carbon and hydrogen isotope systematics of bacterial formation and oxidation of methane. Chem Geol 161:291–314

Whiticar MJ, Faber E, Schoell M (1986) Biogenic methane formation in marine and freshwater environments: CO2 reduction vs. acetate fermentation—isotope evidence. Geochim Cosmochim Acta 50:693–709